A new method for plates with circular holes

C. C. Hsiao　Y. T. Lee　J. T. Chen

Department of Harbor and River Engineering,
National Taiwan Ocean University

Abstract

In this paper, a new method is proposed for plates with circular holes. Null-field integral equation（NFIE）is employed to solve the problem. The kernel in the NFIE is expanded to degenerate kernel and the boundary density is expressed in terms of Fourier series. By matching the boundary condition, a linear algebraic system is obtained. After obtaining the unknown Fourier coefficients, the solution can be obtained by using the integral representation. Finally, an example is presented to demonstrate the validity of present method.

Keywords: plate, null-field integral equation, degenerate kernel, Fourier series

1. INTRODUCTION

Biharmonic problems are always encountered in engineering, e.g. plate problem in solid mechanics and Stokes' flow in fluid mechanics. Although analytical methods involve special mapping technique or restricted solution representations, only a few cases were solved. Numerical methods, finite difference method (FDM), finite element method (FEM) and boundary element method (BEM) [1] have been utilized to solve the problem. For problem with circular boundaries, Fourier series are always incorporated to formulate the solution [2]. The degree of freedom for the nodal value is transformed to the Fourier coefficient.

Based on the null-field integral formulation, we can separate the source and field variables in the fundamental solution for problems with circular boundary. Fourier series for boundary densities are also implemented in the semi-analytical approach [3, 4].

Recently, Shen *et al.* [3, 4] have successfully applied this method to solve Laplace problems with circular holes. We will extend to biharmonic problems in this paper. An annular case is demonstrated to see the validity of the present formulation.

2. PROBLEM STATMENT AND INTEGRAL FORMULATION

Consider the plate problem with circular domain containing N randomly distributed circular holes centered at position vector $\underset{\sim}{c}_j$ ($j=1, 2, \cdots, N$) as shown in Fig. 1. Let a_j denote the radius of the jth circular hole and B_j be the boundary of the circular domain.

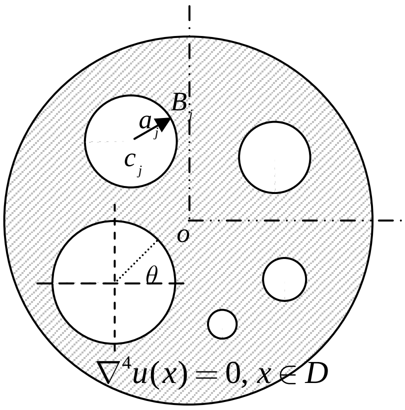

Figure 1 Problem statement

The displacement ($u(\underset{\sim}{s})$), slope ($\theta(\underset{\sim}{s})$), normal moment ($m(\underset{\sim}{s})$), and effective shear force ($v(\underset{\sim}{s})$) on the boundary are approximated by using the Fourier series expansion. Therefore, we have

$$u(\underset{\sim}{s}) = a_{0j} + \sum_{n=1}^{M} (a_{nj} \cos n\theta_j + b_{nj} \sin n\theta_j) \quad , \underset{\sim}{s} \in B_j, \tag{1}$$

$$\theta(\underset{\sim}{s}) = c_{0j} + \sum_{n=1}^{M} (c_{nj} \cos n\theta_j + d_{nj} \sin n\theta_j) \quad , \underset{\sim}{s} \in B_j, \tag{2}$$

$$m(\underset{\sim}{s}) = g_{0j} + \sum_{n=1}^{M} (g_{nj} \cos n\theta_j + h_{nj} \sin n\theta_j) \quad , \underset{\sim}{s} \in B_j, \tag{3}$$

$$v(\underset{\sim}{s}) = p_{0j} + \sum_{n=1}^{M} (p_{nj} \cos n\theta_j + q_{nj} \sin n\theta_j) \quad , \underset{\sim}{s} \in B_j, \tag{4}$$

where a_0, a_{nj}, b_{nj}, c_{nj}, d_{nj}, g_{nj}, h_{nj}, p_{nj} and q_{nj} are the Fourier coefficients, θ_j is the polar angle centered at c_j. Based on the boundary integral formulation of the domain point for the plate problem, the integral equations of plate problem can be derived from the Rayleigh-Green identity as follows：

$$8\pi u(\underset{\sim}{x}) = \int_B \{-U(\underset{\sim}{s},\underset{\sim}{x})v(\underset{\sim}{s}) + \Theta(\underset{\sim}{s},\underset{\sim}{x})m(\underset{\sim}{s}) - M(\underset{\sim}{s},\underset{\sim}{x})\theta(\underset{\sim}{s}) + V(\underset{\sim}{s},\underset{\sim}{x})u(\underset{\sim}{s})\}\, dB(\underset{\sim}{s}), \underset{\sim}{x} \in D \tag{5}$$

$$8\pi \theta(\underset{\sim}{x}) = \int_B \{-U_\theta(\underset{\sim}{s},\underset{\sim}{x})v(\underset{\sim}{s}) + \Theta_\theta(\underset{\sim}{s},\underset{\sim}{x})m(\underset{\sim}{s}) - M_\theta(\underset{\sim}{s},\underset{\sim}{x})\theta(\underset{\sim}{s}) + V_\theta(\underset{\sim}{s},\underset{\sim}{x})u(\underset{\sim}{s})\}\, dB(\underset{\sim}{s}), \underset{\sim}{x} \in D \tag{6}$$

$$8\pi m(\underset{\sim}{x}) = \int_B \{-U_m(\underset{\sim}{s},\underset{\sim}{x})v(\underset{\sim}{s}) + \Theta_m(\underset{\sim}{s},\underset{\sim}{x})m(\underset{\sim}{s}) - M_m(\underset{\sim}{s},\underset{\sim}{x})\theta(\underset{\sim}{s}) + V_m(\underset{\sim}{s},\underset{\sim}{x})u(\underset{\sim}{s})\}\, dB(\underset{\sim}{s}), \underset{\sim}{x} \in D \tag{7}$$

$$8\pi v(\underset{\sim}{x}) = \int_B \{-U_v(\underset{\sim}{s},\underset{\sim}{x})v(\underset{\sim}{s}) + \Theta_v(\underset{\sim}{s},\underset{\sim}{x})m(\underset{\sim}{s}) - M_v(\underset{\sim}{s},\underset{\sim}{x})\theta(\underset{\sim}{s}) + V_v(\underset{\sim}{s},\underset{\sim}{x})u(\underset{\sim}{s})\}\, dB(\underset{\sim}{s}), \underset{\sim}{x} \in D \tag{8}$$

The degenerate kernels for the sixteen kernel functions are defined as shown in Fig. 2

$$\begin{array}{cccccccc}
U(\underset{\sim}{s},\underset{\sim}{x}) & \xrightarrow{K_{\theta,s}(\cdot)} & \Theta(\underset{\sim}{s},\underset{\sim}{x}) & \xrightarrow{K_{m,s}(\cdot)} & M(\underset{\sim}{s},\underset{\sim}{x}) & \xrightarrow{K_{v,s}(\cdot)} & V(\underset{\sim}{s},\underset{\sim}{x}) & \\
 & & & & & & \downarrow & K_{\theta,x}(\cdot) \\
U_\theta(\underset{\sim}{s},\underset{\sim}{x}) & & \Theta_\theta(\underset{\sim}{s},\underset{\sim}{x}) & & M_\theta(\underset{\sim}{s},\underset{\sim}{x}) & & V_\theta(\underset{\sim}{s},\underset{\sim}{x}) & \\
 & & & & & & \downarrow & K_{m,x}(\cdot) \\
U_m(\underset{\sim}{s},\underset{\sim}{x}) & & \Theta_m(\underset{\sim}{s},\underset{\sim}{x}) & & M_m(\underset{\sim}{s},\underset{\sim}{x}) & & V_m(\underset{\sim}{s},\underset{\sim}{x}) & \\
 & & & & & & \downarrow & K_{v,x}(\cdot) \\
U_v(\underset{\sim}{s},\underset{\sim}{x}) & & \Theta_v(\underset{\sim}{s},\underset{\sim}{x}) & & M_v(\underset{\sim}{s},\underset{\sim}{x}) & & V_v(\underset{\sim}{s},\underset{\sim}{x}) &
\end{array}$$

Figure 2 The relationship between the sixteen degenerate kernels

where the operators $K_{\theta,s}(\cdot)$, $K_{m,s}(\cdot)$, and $K_{v,s}(\cdot)$ are defined by

$$K_{\theta,s}(\cdot) = \frac{\partial(\cdot)}{\partial n_s} \tag{9}$$

$$K_{m,s}(\cdot)=\nu\nabla^2(\cdot)+(1-\nu)\frac{\partial^2(\cdot)}{\partial n_s} \tag{10}$$

$$K_{v,s}(\cdot)=\frac{\partial\nabla^2(\cdot)}{\partial n_s}+(1-\nu)\frac{\partial}{\partial t_s}\left[\frac{\partial}{\partial n_s}\left(\frac{\partial(\cdot)}{\partial t_s}\right)\right] \tag{11}$$

where $\underset{\sim}{s}$ and $\underset{\sim}{x}$ are the source and field points, respectively. n_s and t_s denote the outward normal vector and tangential vector at the source point s, respectively, D is the domain of interest, B is the boundary, ν is the Poisson ratio and $U(\underset{\sim}{s},\underset{\sim}{x})=r^2\ln r$ is the fundamental solution which satisfies

$$\nabla^4 U(\underset{\sim}{s},\underset{\sim}{x})=8\pi\delta(\underset{\sim}{s}-\underset{\sim}{x}) \tag{12}$$

where, $\delta(\underset{\sim}{s}-\underset{\sim}{x})$ denotes the Dirac-delta function and r is the distance between source point and field point. By collocating $\underset{\sim}{x}$ outside the domain ($\underset{\sim}{x}\in D^e$), the null-field integral equation can be obtained as shown below

$$0=\int_B\{-U(s,x)v(s)+\Theta(s,x)m(s)-M(s,x)\theta(s)+V(s,x)u(s)\}\,dB(s),\quad x\in D^e, \tag{13}$$

$$0=\int_B\{-U_\theta(s,x)v(s)+\Theta_\theta(s,x)m(s)-M_\theta(s,x)\theta(s)+V_\theta(s,x)u(s)\}\,dB(s),\quad x\in D^e, \tag{14}$$

$$0=\int_B\{-U_m(s,x)v(s)+\Theta_m(s,x)m(s)-M_m(s,x)\theta(s)+V_m(s,x)u(s)\}\,dB(s),\quad x\in D^e, \tag{15}$$

$$0=\int_B\{-U_v(s,x)v(s)+\Theta_v(s,x)m(s)-M_v(s,x)\theta(s)+V_v(s,x)u(s)\}\,dB(s),\quad x\in D^e, \tag{16}$$

Based on the separable property, sixteen kernel functions can be expanded into degenerate form as shown in the appendix, where ρ indicates $|\underset{\sim}{x}-\underset{\sim}{c}_j|$, R denotes $|\underset{\sim}{s}-\underset{\sim}{c}_j|$, and α is the angle between $\underset{\sim}{x}-\underset{\sim}{c}_j$ and $\underset{\sim}{s}-\underset{\sim}{c}_j$, and the superscripts "$i$" and "$e$" denote the interior and exterior cases, respectively. In the real computation, only finite M terms are used in the summation of Eqs. (1) and (2).

3. LINEAR ALGEBRAIC SYSTEM

By collocating the null-field point $|\underset{\sim}{x}_k-\underset{\sim}{c}_j|=a_k^-$ on the $k\,th$ circular boundary for Eqs. (13) and (14), we have

$$0=\sum_{j=1}^{N_c}\int_B\{-U(\underset{\sim}{s},\underset{\sim}{x}_k)v(\underset{\sim}{s})+\Theta(\underset{\sim}{s},\underset{\sim}{x}_k)m(\underset{\sim}{s})-M(\underset{\sim}{s},\underset{\sim}{x}_k)\theta(\underset{\sim}{s})+V(\underset{\sim}{s},\underset{\sim}{x}_k)u(\underset{\sim}{s})\}\,dB(\underset{\sim}{s}),\quad \underset{\sim}{x}\in D^e, \tag{17}$$

$$0=\sum_{j=1}^{N_c}\int_B\{-U_\theta(\underset{\sim}{s},\underset{\sim}{x}_k)v(\underset{\sim}{s})+\Theta_\theta(\underset{\sim}{s},\underset{\sim}{x}_k)m(\underset{\sim}{s})-M_\theta(\underset{\sim}{s},\underset{\sim}{x}_k)\theta(\underset{\sim}{s})+V_\theta(\underset{\sim}{s},\underset{\sim}{x}_k)u(\underset{\sim}{s})\}\,dB(\underset{\sim}{s}),\quad \underset{\sim}{x}\in D^e, \tag{18}$$

where N_c is the number of circles. It is noted that the path is counterclockwise for the outer circle. Otherwise, it is clockwise.

For the B_j integral of the circular boundary, the degenerate kernels of $U(\underset{\sim}{s},\underset{\sim}{x})$, $\Theta(\underset{\sim}{s},\underset{\sim}{x})$, $M(\underset{\sim}{s},\underset{\sim}{x})$, and $V(\underset{\sim}{s},\underset{\sim}{x})$ in the appendix are utilized. $u(s)$, $\theta(s)$, $m(s)$, and $v(s)$ are substituted by using the Fourier series of Eqs. (1) − (4), respectively.

In the B_j integration, we set the origin of the observer system to collocate at the center c_j to fully utilize the degenerate kernel and Fourier series. By collocating the null-field point near B_k, Fig. 3(a) shows the collocation point and boundary contour. A linear algebraic system is obtained

$$[A]\{x\}=[B]\{y\} \tag{19}$$

where $[A]=\begin{bmatrix} U & \Theta \\ U_\theta & \Theta_\theta \end{bmatrix}$, $[B]=\begin{bmatrix} M & V \\ M_\theta & V_\theta \end{bmatrix}$, $[A]$ and $[B]$ are the influence matrices, $\{x\}$ and $\{y\}$ denote the vectors of Fourier coefficients for $u(s)$, $\theta(s)$, $m(s)$, and $v(s)$, respectively. By rearranging the known and unknown sets, the unknown Fourier coefficients are determined. After obtaining the unknown Fourier coefficients, the origin of observer system is set to c_j in the B_j integration as shown in Fig. 3(b) to obtain the interior potential by employing Eq. (5). The flow chart of the present method is shown in Fig. 4.

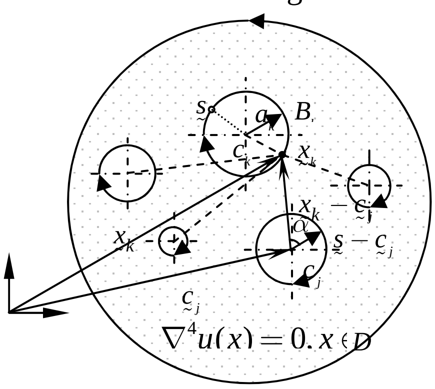

Figure 3(a) Null-field integral equation

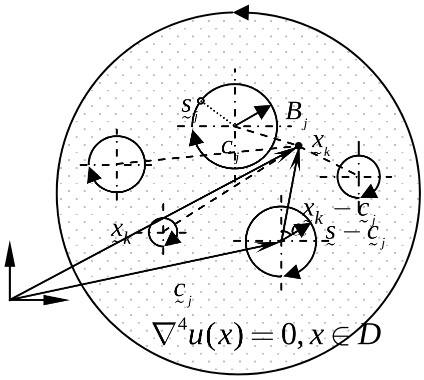

Figure 3(b) Boundary integral equation for the domain point

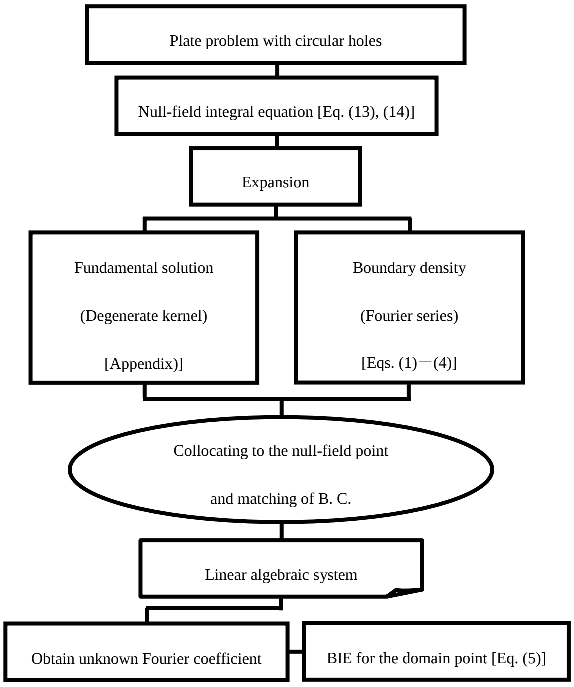

Figure 4 The flow chart of the present method

4. A NUMERICAL EXAMPLE

In order to demonstrate the validity of the present method. One example is given. An annular case with radii a_1 and a_2 ($a_1=1$, $a_2=2$) is shown in Fig. 5 (a). The boundary conditions on the inner boundary are $u_1(\underset{\sim}{s})=-3\sin\theta$, $\theta_1(\underset{\sim}{s})=-5\sin\theta$ and the boundary conditions on the outer boundary are $u_2(\underset{\sim}{s})=0$, $\theta_2(\underset{\sim}{s})=2\sin\theta$. The unknown boundary densities are expanded by the Fourier series and the numerical results are shown in Fig. 5(b), 5(d). The contour of potential is shown in Fig. 6(a). Good agreement is made after comparing with the exact solution [5],

$$u(\rho,\phi)=\rho\sin\phi-\frac{4}{\rho}\sin\phi \qquad (20)$$

as shown in Fig. 6(b).

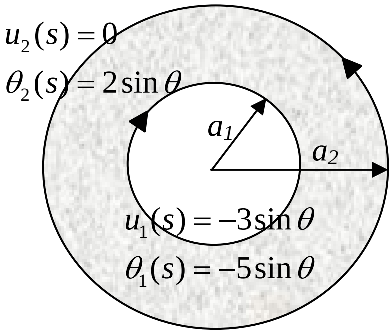

Figure 5(a) An annular problem

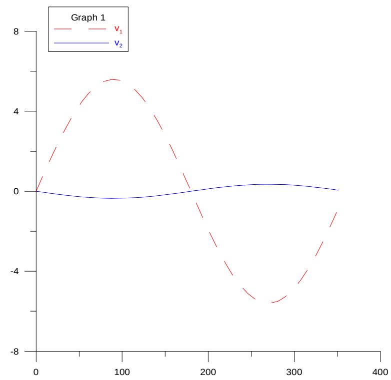

Figure 5(b) The numerical solution of boundary densities of $v(s)$

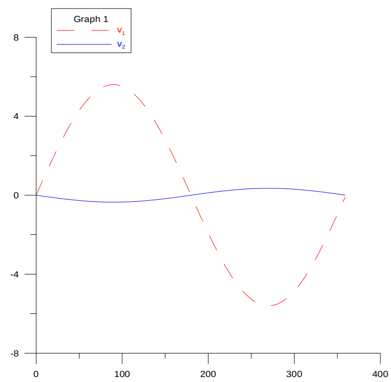

Figure 5(c) The exact solution of boundary densities of $v(s)$

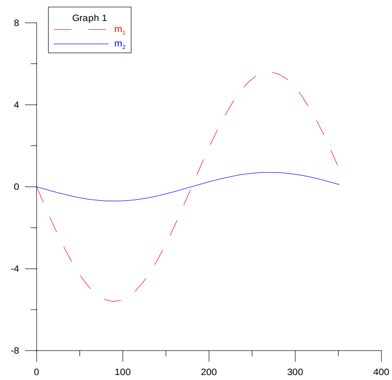

Figure 5(d) The numerical solution of boundary densities of $m(s)$

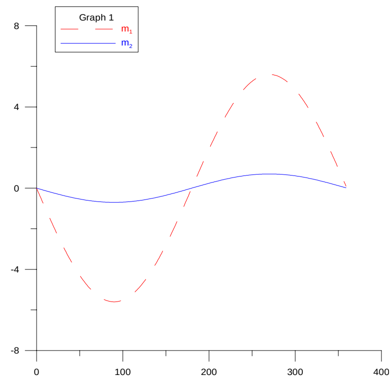

Figure 5(e) The exact solution of boundary densities of $m(s)$

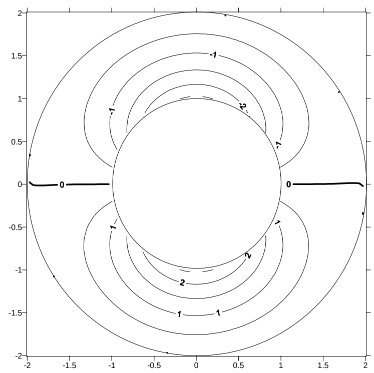

Figure 6(a) Contour of potential (M=10)

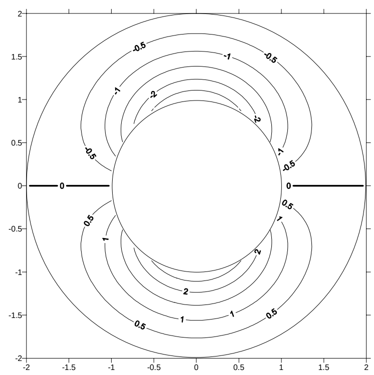

Figure 6(b) Exact solution [5]

In the example, only ten terms of Fourier series (M=10) were needed to converge well with the exact solution [5].

5. CONCLUSIONS

For the plate problems with circular boundaries, we have proposed a special BIEM by using degenerate kernels, null-field integral equation and Fourier series in an adaptive observer system. Numerical results agree very well with the exact solution. It can be easily extended to problems with multiple holes.

ACKNOWLEDGEMENT

Financial support from the Nation Science Council under Grant No. NSC-93-2211-E-019-010 for Nation Taiwan Ocean University is gratefully acknowledged.

REFERENCES

1. 陳正宗與洪宏基, “邊界元素法”, 第二版, 新世界出版社, 台北, (1992).
2. Bird, M. D. and Steele, C. R., “Separated Solution Procedure for Bending of Circular Plates with Circular Holes”, Applied Mechanics Reviews, Vol. 44, pp. 27-35, (1991).
3. Shen, W. C., Lee, C. F. and Chen, J. T., “A Study on Half-Plane Laplace Problems with a Circular Hole”, The 7th National Conference on Structure Engineering, Chung-Li, (2004).
4. Shen, W. C., Lee, C. F. and Chen, J. T., “A study on Laplace Problems of Infinite Plane with Multiple Circular Holes”, The International Conference on Computational Methods, Singapore, (2004)
5. Wu, C. S., Degenerate scale analysis for membrane and plate problems using the meshless method and boundary element method, Master Thesis, Department of Harbor and River Engineering, National Taiwan Ocean University, Keelung, Taiwan, (2004).

二維區域含圓洞之
板問題的新解法

蕭嘉俊 李應德　陳正宗
國立台灣海洋大學河海工程學系

摘要

本文提出一套求解含圓孔洞板問題之新方法。將核函數展開成退化核，而未知的邊界密度函數則由傅立葉級數做展開，利用上述方法可導得一線性代數系統以求得邊界資訊，透過域內點積分方程即可求得場解表示式。最後提出一個測試例以驗證此法之可行性。

關鍵字：板振動，零場積分方程式，退化核，傅立葉級數

Appendix Degenerate kernels for the sixteen kernel functions

$$U(s,x)=\begin{cases} U^I(s,x)=\rho^2(1+\ln R)+R^2\ln R-R\rho(1+2\ln R)\cos(\theta-\phi)-\sum\limits_{m=1}^{\infty}\dfrac{1}{m(m+1)}\dfrac{\rho^{m+2}}{R^m}\cos[m(\theta-\phi)]+\sum\limits_{m=2}^{\infty}\dfrac{1}{m(m-1)}\dfrac{\rho^m}{R^{m-2}}\cos[m(\theta-\phi)],\ R>\rho \\ U^E(s,x)=R^2(1+\ln\rho)+\rho^2\ln\rho-\rho R(1+2\ln\rho)\cos(\theta-\phi)-\sum\limits_{m=1}^{\infty}\dfrac{1}{m(m+1)}\dfrac{R^{m+2}}{\rho^m}\cos[m(\theta-\phi)]+\sum\limits_{m=2}^{\infty}\dfrac{1}{m(m-1)}\dfrac{R^m}{\rho^{m-2}}\cos[m(\theta-\phi)],\ \rho>R \end{cases}$$

$$U_\theta(s,x)=\begin{cases} U_\theta^I(s,x)=2\rho(1+\ln R)-R(1+2\ln R)\cos(\theta-\phi)-\sum\limits_{m=1}^{\infty}\dfrac{m+2}{m(m+1)}\dfrac{\rho^{m+1}}{R^m}\cos[m(\theta-\phi)]+\sum\limits_{m=2}^{\infty}\dfrac{1}{m-1}\dfrac{\rho^{m-1}}{R^{m-2}}\cos[m(\theta-\phi)],\ R>\rho \\ U_\theta^E(s,x)=\dfrac{R^2}{\rho}+\rho(1+2\ln\rho)-R(3+2\ln\rho)\cos(\theta-\phi)+\sum\limits_{m=1}^{\infty}\dfrac{1}{m+1}\dfrac{R^{m+2}}{\rho^{m+1}}\cos[m(\theta-\phi)]-\sum\limits_{m=2}^{\infty}\dfrac{m-2}{m(m-1)}\dfrac{R^m}{\rho^{m-1}}\cos[m(\theta-\phi)],\ \rho>R \end{cases}$$

$$U_m(s,x)=\begin{cases} U_m^I(s,x)=2(1+\nu)(1+\ln R)+\sum\limits_{m=1}^{\infty}\dfrac{m(\nu-1)-2(\nu+1)}{m}\dfrac{\rho^m}{R^m}\cos[m(\theta-\phi)]+\sum\limits_{m=2}^{\infty}(1-\nu)\dfrac{\rho^{m-2}}{R^{m-2}}\cos[m(\theta-\phi)],\ R>\rho \\ U_m^E(s,x)=\dfrac{R^2}{\rho^2}(\nu-1)+(3+2\ln\rho)+\nu(1+2\ln\rho)-\dfrac{2R}{\rho}(1+\nu)\cos(\theta-\phi)+\sum\limits_{m=1}^{\infty}(\nu-1)\dfrac{R^{m+2}}{\rho^{m+2}}\cos[m(\theta-\phi)]+\sum\limits_{m=2}^{\infty}\dfrac{m(1-\nu)-2(1+\nu)}{m}\dfrac{R^m}{\rho^m}\cos[m(\theta-\phi)],\ \rho>R \end{cases}$$

$$U_v(s,x)=\begin{cases} U_v^I(s,x)=\sum\limits_{m=1}^{\infty}(m-4-m\nu)\dfrac{\rho^{m-1}}{R^m}\cos[m(\theta-\phi)]+\sum\limits_{m=2}^{\infty}m(1-\nu)\dfrac{\rho^{m-3}}{R^{m-2}}\cos[m(\theta-\phi)],\ R>\rho \\ U_v^E(s,x)=\dfrac{4}{\rho}+\sum\limits_{m=1}^{\infty}m(\nu-1)\dfrac{R^{m+2}}{\rho^{m+3}}\cos[m(\theta-\phi)]+\sum\limits_{m=2}^{\infty}(-m\nu+m+4)\dfrac{R^m}{\rho^{m+1}}\cos[m(\theta-\phi)],\ \rho>R \end{cases}$$

$$\Theta(s,x)=\begin{cases} \Theta^I(s,x)=\dfrac{\rho^2}{R}+R(1+2\ln R)-\rho(3+2\ln R)\cos(\theta-\phi)+\sum\limits_{m=1}^{\infty}\dfrac{1}{m+1}\dfrac{\rho^{m+2}}{R^{m+1}}\cos[m(\theta-\phi)]-\sum\limits_{m=2}^{\infty}\dfrac{m-2}{m(m-1)}\dfrac{\rho^m}{R^{m-1}}\cos[m(\theta-\phi)],\ R>\rho \\ \Theta^E(s,x)=2R(1+\ln\rho)-\rho(1+2\ln\rho)\cos(\theta-\phi)-\sum\limits_{m=1}^{\infty}\dfrac{m+2}{m(m+1)}\dfrac{R^{m+1}}{\rho^m}\cos[m(\theta-\phi)]+\sum\limits_{m=2}^{\infty}\dfrac{1}{m-1}\dfrac{R^{m-1}}{\rho^{m-2}}\cos[m(\theta-\phi)],\ \rho>R \end{cases}$$

$$\Theta_\theta(s,x)=\begin{cases} \Theta_\theta^I(s,x)=\dfrac{2\rho}{R}-(3+2\ln R)\cos(\theta-\phi)+\sum\limits_{m=1}^{\infty}\dfrac{m+2}{m+1}\dfrac{\rho^{m+1}}{R^{m+1}}\cos[m(\theta-\phi)]-\sum\limits_{m=2}^{\infty}\dfrac{m-2}{m-1}\dfrac{\rho^{m-1}}{R^{m-1}}\cos[m(\theta-\phi)],\ R>\rho \\ \Theta_\theta^E(s,x)=\dfrac{2R}{\rho}-(3+2\ln\rho)\cos(\theta-\phi)+\sum\limits_{m=1}^{\infty}\dfrac{m+2}{m+1}\dfrac{R^{m+1}}{\rho^{m+1}}\cos[m(\theta-\phi)]-\sum\limits_{m=2}^{\infty}\dfrac{m-2}{m-1}\dfrac{R^{m-1}}{\rho^{m-1}}\cos[m(\theta-\phi)],\ \rho>R \end{cases}$$

$$\Theta_m(s,x)=\begin{cases} \Theta_m^I(s,x)=\dfrac{2}{R}(1+\nu)-\sum\limits_{m=1}^{\infty}[m(\nu-1)-2(\nu+1)]\dfrac{\rho^m}{R^{m+1}}\cos[m(\theta-\phi)]-\sum\limits_{m=2}^{\infty}(1-\nu)(m-2)\dfrac{\rho^{m-2}}{R^{m-1}}\cos[m(\theta-\phi)],\ R>\rho \\ \Theta_m^E(s,x)=\dfrac{2R}{\rho^2}(\nu-1)-\dfrac{2}{\rho}(1+\nu)\cos(\theta-\phi)+\sum\limits_{m=1}^{\infty}(m+2)(\nu-1)\dfrac{R^{m+1}}{\rho^{m+2}}\cos[m(\theta-\phi)]+\sum\limits_{m=2}^{\infty}(m(1-\nu)-2(1+\nu))\dfrac{R^{m-1}}{\rho^m}\cos[m(\theta-\phi)],\ \rho>R \end{cases}$$

$$\Theta_v(s,x)=\begin{cases} \Theta_v^I(s,x)=-\sum\limits_{m=1}^{\infty}m(m-4-m\nu)\dfrac{\rho^{m-1}}{R^{m+1}}\cos[m(\theta-\phi)]-\sum\limits_{m=2}^{\infty}m(m-2)(1-\nu)\dfrac{\rho^{m-3}}{R^{m-1}}\cos[m(\theta-\phi)],\ R>\rho \\ \Theta_v^E(s,x)=\sum\limits_{m=1}^{\infty}m(m+2)(\nu-1)\dfrac{R^{m+1}}{\rho^{m+3}}\cos[m(\theta-\phi)]+\sum\limits_{m=2}^{\infty}m(-m\nu+m+4)\dfrac{R^{m-1}}{\rho^{m+1}}\cos[m(\theta-\phi)],\ \rho>R \end{cases}$$

$$M(s,x)=\begin{cases} M^I(s,x)=(\nu-1)\dfrac{\rho^2}{R^2}+(\nu+3)+2(\nu+1)\ln R-(\nu+1)\dfrac{2\rho}{R}\cos(\theta-\phi)+\sum\limits_{m=1}^{\infty}(\nu-1)\dfrac{\rho^{m+2}}{R^{m+2}}\cos[m(\theta-\phi)]+\sum\limits_{m=2}^{\infty}\dfrac{m(1-\nu)-2(1+\nu)}{m}\dfrac{\rho^m}{R^m}\cos[m(\theta-\phi)],\ R>\rho \\ M^E(s,x)=2(1+\nu)(1+\ln\rho)+\sum\limits_{m=1}^{\infty}\dfrac{m(\nu-1)-2(\nu+1)}{m}\dfrac{R^m}{\rho^m}\cos[m(\theta-\phi)]+\sum\limits_{m=2}^{\infty}(1-\nu)\dfrac{R^{m-2}}{\rho^{m-2}}\cos[m(\theta-\phi)],\ \rho>R \end{cases}$$

$$M_\theta(s,x)=\begin{cases} M_\theta^I(s,x)=\dfrac{2\rho(\nu-1)}{R^2}-\dfrac{2(\nu+1)}{R}\cos(\theta-\phi)+\sum\limits_{m=1}^{\infty}(\nu-1)(m+2)\dfrac{\rho^{m+1}}{R^{m+2}}\cos[m(\theta-\phi)]+\sum\limits_{m=2}^{\infty}[m(1-\nu)-2(1+\nu)]\dfrac{\rho^{m-1}}{R^m}\cos[m(\theta-\phi)],\ R>\rho \\ M_\theta^E(s,x)=\dfrac{2(1+\nu)}{\rho}-\sum\limits_{m=1}^{\infty}(m(\nu-1)-2(\nu+1))\dfrac{R^m}{\rho^{m+1}}\cos[m(\theta-\phi)]+\sum\limits_{m=2}^{\infty}((1-\nu)(-m+2))\dfrac{R^{m-2}}{\rho^{m-1}}\cos[m(\theta-\phi)],\ \rho>R \end{cases}$$

$$M_m(s,x)=\begin{cases} M_m^I(s,x)=\dfrac{2(\nu^2-1)}{R^2}+\sum\limits_{m=1}^{\infty}(m(\nu-1)-2(\nu+1))(m+1)(1-\nu)\dfrac{\rho^m}{R^{m+2}}\cos[m(\theta-\phi)]+\sum\limits_{m=2}^{\infty}(1-\nu)(m-1)(m(1-\nu)-2(\nu+1))\dfrac{\rho^{m-2}}{R^m}\cos[m(\theta-\phi)],\ R>\rho \\ M_m^E(s,x)=\dfrac{2(\nu^2-1)}{\rho^2}+\sum\limits_{m=1}^{\infty}(m(\nu-1)-2(\nu+1))(m+1)(1-\nu)\dfrac{R^m}{\rho^{m+2}}\cos[m(\theta-\phi)]+\sum\limits_{m=2}^{\infty}(1-\nu)(m-1)(m(1-\nu)-2(\nu+1))\dfrac{R^{m-2}}{\rho^m}\cos[m(\theta-\phi)],\ \rho>R \end{cases}$$

$$M_v(s,x)=\begin{cases} M_v^I(s,x)=\sum\limits_{m=1}^{\infty}m(m+1)(1-\nu)[m(1-\nu)-4]\dfrac{\rho^{m-1}}{R^{m+2}}\cos[m(\theta-\phi)]+\sum\limits_{m=2}^{\infty}(1-\nu)m(m-1)[m(1-\nu)-2(1+\nu)]\dfrac{\rho^{m-3}}{R^m}\cos[m(\theta-\phi)],\ R>\rho \\ M_v^E(s,x)=\sum\limits_{m=1}^{\infty}m(m+1)(1-\nu)(m(\nu-1)-2(\nu+1))\dfrac{R^m}{\rho^{m+3}}\cos[m(\theta-\phi)]+\sum\limits_{m=2}^{\infty}(1-\nu)m(m-1)(m(1-\nu)+4)\dfrac{R^{m-2}}{\rho^{m+1}}\cos[m(\theta-\phi)],\ \rho>R \end{cases}$$

$$V(s,x)=\begin{cases} V^I(s,x)=\dfrac{4}{R}+\sum_{m=1}^{\infty} m(\nu-1)\dfrac{\rho^{m+2}}{R^{m+3}}\cos[m(\theta-\phi)]+\sum_{m=2}^{\infty}(m+4-m\nu)\dfrac{\rho^{m}}{R^{m+1}}\cos[m(\theta-\phi)],\ R>\rho \\ V^E(s,x)=\sum_{m=1}^{\infty}(m(1-\nu)-4)\dfrac{R^{m-1}}{\rho^{m}}\cos[m(\theta-\phi)]+\sum_{m=2}^{\infty} m(1-\nu)\dfrac{R^{m-3}}{\rho^{m-2}}\cos[m(\theta-\phi)],\ \rho>R \end{cases}$$

$$V_\theta(s,x)=\begin{cases} V_\theta^I(s,x)=\sum_{m=1}^{\infty} m(m+2)(\nu-1)\dfrac{\rho^{m+1}}{R^{m+3}}\cos[m(\theta-\phi)]+\sum_{m=2}^{\infty} m(m+4-m\nu)\dfrac{\rho^{m-1}}{R^{m+1}}\cos[m(\theta-\phi)],\ R>\rho \\ V_\theta^E(s,x)=-\sum_{m=1}^{\infty} m(m(1-\nu)-4)\dfrac{R^{m-1}}{\rho^{m+1}}\cos[m(\theta-\phi)]+\sum_{m=2}^{\infty} m(-m+2)(1-\nu)\dfrac{R^{m-3}}{\rho^{m-1}}\cos[m(\theta-\phi)],\ \rho>R \end{cases}$$

$$V_m(s,x)=\begin{cases} V_m^I(s,x)=\sum_{m=1}^{\infty} m(m+1)(1-\nu)[m(\nu-1)-2(\nu+1)]\dfrac{\rho^{m}}{R^{m+3}}\cos[m(\theta-\phi)]+\sum_{m=2}^{\infty} m(m-1)(1-\nu)[m(1-\nu)+4]\dfrac{\rho^{m-2}}{R^{m+1}}\cos[m(\theta-\phi)],\ R>\rho \\ V_m^E(s,x)=\sum_{m=1}^{\infty} m(m+1)(1-\nu)(m(1-\nu)-4)\dfrac{R^{m-1}}{\rho^{m+2}}\cos[m(\theta-\phi)]+\sum_{m=2}^{\infty} m(m-1)(1-\nu)(m(1-\nu)-2(\nu+1))\dfrac{R^{m-3}}{\rho^{m}}\cos[m(\theta-\phi)],\ \rho>R \end{cases}$$

$$V_v(s,x)=\begin{cases} V_v^I(s,x)=\sum_{m=1}^{\infty} m^2(m+1)(1-\nu)[m(1-\nu)-4]\dfrac{\rho^{m-1}}{R^{m+3}}\cos[m(\theta-\phi)]+\sum_{m=2}^{\infty} m^2(m-1)(1-\nu)(m(1-\nu)+4)\dfrac{\rho^{m-3}}{R^{m+1}}\cos[m(\theta-\phi)],\ R>\rho \\ V_v^E(s,x)=\sum_{m=1}^{\infty} m^2(m+1)(1-\nu)(m(1-\nu)-4)\dfrac{R^{m-1}}{\rho^{m+3}}\cos[m(\theta-\phi)]+\sum_{m=2}^{\infty} m^2(m-1)(1-\nu)(m(1-\nu)+4)\dfrac{R^{m-3}}{\rho^{m+1}}\cos[m(\theta-\phi)],\ \rho>R \end{cases}$$

Interior:

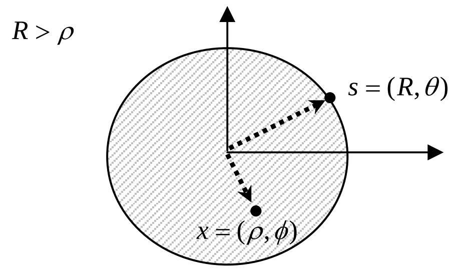

Exterior: